Supplementary Information for

Does ambient secondary conversion or the prolonged fast conversion in combustion plumes cause severe $PM_{2.5}$ air pollution in China?

Yanjie Shen, He Meng, Xiaohong Yao*, Zhong-Ren Peng, Yele Sun, Jie Zhang, Yang Gao, Limin Feng, Xiaohuan Liu, Huiwang Gao

*Corresponding author: Xiaohong Yao

Email: xhyao@ouc.edu.cn

This file includes:

Supplementary text

Figures S1–S10

Legends for Videos S1–S6

Supplementary Information Text

Negligible contribution from ambient FSPM to significant increase in $PM_{2.5}$ at Wanliu site

At the Wanliu site in Beijing on 13 January 2019, no detectable contribution from ambient FSPM to the significant increase in $PM_{2.5}$ can be found during the period from 17:00 to 23:00 (blue markers in Fig. 3d, $PM_{2.5}$/CO=74 ± 7 μg m^{-3}/mg m^{-3}). The replacement process occurred within 1 h before the accumulation, that is, two variables sharply changed from 11 μg m^{-3} and 16 μg m^{-3} / mg m^{-3} at 16:00 to 87 μg m^{-3} and 67 μg m^{-3}/mg m^{-3} at 17:00.

A long replacement process likely occurred from the afternoon on 12 January to the morning on 13 January. We further plotted the theoretical dilution curve, that is, the gray dashed line in Fig. 3e, using the same approach used for Tiantan and selecting two end points, that is, one was at 20:00 on 12 January with the maximum $PM_{2.5}$ hourly average of 574 μg m^{-3} and the maximum ratio of 120 μg m^{-3}/mg m^{-3} to be observed; the other was at 11:00 on 13 January with the hourly average of $PM_{2.5}$ and the ratio as low as 7 μg m^{-3} and 14 μg m^{-3}/mg m^{-3}, respectively. The red shadowed area represents the existence of ambient FSPM during the dilution period. The observational data during the dilution period were far below the gray line, as shown in Fig. 3e, indicating that the evaporation of semi-volatile species from $PM_{2.5}$ took place rather than ambient FSPM.

The pink dashed line represents the theoretical replacement curve during the period with increasing $PM_{2.5}$ from 124 μg m^{-3} at 13:00 to the maximum value. The line was above the observational data during the period, allowing us to reject the null hypothesis of the detectable contribution from ambient FSPM. Again, strong correlations between the ratios of $PM_{2.5}/CO$ and mass concentrations of $PM_{2.5}$ can be obtained during the increasing (red markers) and decreasing periods (black markers) due to mixing, that is, $[PM_{2.5}/CO] = 0.15 \times [PM_{2.5}]+38$, $R^2 = 0.99$, $P < 0.01$, for the former and $[PM_{2.5}/CO] = 0.12 \times [PM_{2.5}]+43$, $R^2 = 0.95$, $P < 0.01$, for the latter. When the data during the whole study period at Wanliu were used for the regression, we obtained $[PM_{2.5}/CO] = 0.17 \times [PM_{2.5}]+29$, $R^2 = 0.85$, $P < 0.01$ (Fig. 3e). The decrease in the R^2 value is ascribed to varying mixing rates in different periods.

Negligible contribution from ambient FSPM to significant increase in $PM_{2.5}$ in Langfang

The negligible contribution from ambient FSPM can also be found in Langfang when time series of hourly averages of $PM_{2.5}$ and the ratios of $PM_{2.5}/CO$ were examined during the episodic period (Fig. S4a). On the first platform of $PM_{2.5}/CO$ (red markers), the hourly averages of $PM_{2.5}$ increased largely by 117 % (from 59 μg m^{-3} at 21:00 on 9 January to 128 μg m^{-3} at 09:00 on 10 January) and then decreased by 9 % until 11:00 on 10 January ($PM_{2.5}$= 117 μg m^{-3}). The ratios of $PM_{2.5}/CO$ narrowly fluctuated at approximately 55±3 μg m^{-3}/mg m^{-3} (3/55 = 5.5 %). After a 2 h transition, the ratios of $PM_{2.5}/CO$ stood on a higher platform (pink markers) and fluctuated narrowly at approximately 75±3 μg m^{-3}/mg m^{-3} (3/75 = 4.0 %) with hourly averages of $PM_{2.5}$, which increased by 67 % from 14:00 on 10 January ($PM_{2.5}$ = 118 μg m^{-3}) to 01:00 on 11 January ($PM_{2.5}$ = 197 μg m^{-3}). After this, orange markers exhibited another replacement process, followed by the accumulation of $PM_{2.5}$, with a negligible contribution from ambient FSPM.

The accumulation accompanied by the evaporation of semi-volatile species from $PM_{2.5}$

can be identified from 19:00 on 12 January to 06:00 on 13 January (half green markers). During this period, the concentrations of $PM_{2.5}$ fluctuated narrowly around 275±11 μg m^{-3} (11/275 ≈ 4 %), whereas the ratios of $PM_{2.5}$/CO exhibited a decreasing trend of approximately 30 % (from 103 μg m^{-3}/mg m^{-3} to 72 μg m^{-3}/mg m^{-3}).

The hourly averages of $PM_{2.5}$ fluctuated narrowly around 268±10 μg m^{-3} (10/268 = 3.7 %) from 18:00 on 11 January to 07:00 on 12 January (half blue markers). The ratios of $PM_{2.5}$/CO increased first and then decreased. During the decreasing period of $PM_{2.5}$/CO, the evaporation of semi-volatile species from $PM_{2.5}$ also probably occurred.

A moderately good correlation can be obtained here also, that is, [$PM_{2.5}$/CO] = 0.17 × [$PM_{2.5}$]+40, $R^2 = 0.75$, $P < 0.01$, when all data during the study period were used. The lower R^2 value may also be ascribed to different mixing rates of plumes.

Monitoring particle formation in fresh stack combustion plumes

We assemble a nano-Scan Particle Sizer (SMPS, Model 3910, TSI corporation, USA) on an Unmanned Aerial Vehicle developed in 2017 (UAV, PloughUAV Corporation, China), to monitor the particle formation in fresh stack combustion plumes (see Supplementary video 6). The height of large stacks is typically 200-500 m. The SMPS takes one minute each time to scan from 10 nm to 420 nm of particle size. In fresh stack combustion plumes, the SMPS practically needs full-spectrum scans as more as possible to obtain credible average results. The newly developed UAV has a payload of 20 kg and flight time of 20 minutes. This allows the SMPS, the lightest commercial nano-particle sizer (9 kg), available to have a reasonable time to measure the particle number concentrations in fresh plumes by deducting the take-off and landing times. Fig. S10 shows the measurement results made in the morning (07:15-07:28) and afternoon

(14:37-14:47) on 22 December 2017 (300 m height stacks in Shanghai, 31.460° N, 121.421° E). Each cruise lasted for approximately 15 minutes, including lifting, suspending for measurements and landing. The other UAV (Phantom-4, DJI Corporation, China) with a camera was used to record flying process with the UAV carrying the SMPS.

In the morning cruise, the measured number concentrations in the ambient air were $2.6\pm1.0\times10^{4}$ cm^{-3}. The values reduced to $9.5\pm5.9\times10^{3}$ cm^{-3} in the fresh stack combustion plumes when the UAV suspended for measurement. Meanwhile, the geometric median diameter (GMD) of atmospheric particles increased from 59±7 nm in the ambient air to 94±6 nm in the fresh stack combustion plumes. See in the Fig. S10a. Since the effective correction method is still underdeveloped, the total particle number concentrations may suffer from the artifact due to the reduced sampling flow rate during the cruise. However, the artifact may exert a minor influence on the particle number size distribution pattern. Non-precipitation cloud droplets in fresh plumes played an important role in transferring smaller particles into the >80 nm particle via Hoppel effect, increasing the particle size while decreasing Aitken mode particle number concentration. Relative humidity (RH) in the morning cruising was 91 % while wind speed (WS) was 0 m/s, indicated that the background air was humid and stable. In the afternoon cruise, see in the Fig. S10b, the measured number concentrations in the ambient air was $2.7\pm1.8\times10^{4}$ cm^{-3} and the values in the fresh plumes were $2.8\pm0.6\times10^{4}$ cm^{-3}. Compared with the measurements in the morning, more Aitken mode particles were observed in the afternoon's fresh plumes. More rapid depletion of water droplets in the afternoon because of low RH (32 %) lead to a lower scavenging efficiency for the Aitken mode particles. The lifetime of water droplets in the fresh plumes appears to play a critical role in determining the particle number concentrations and size distributions.

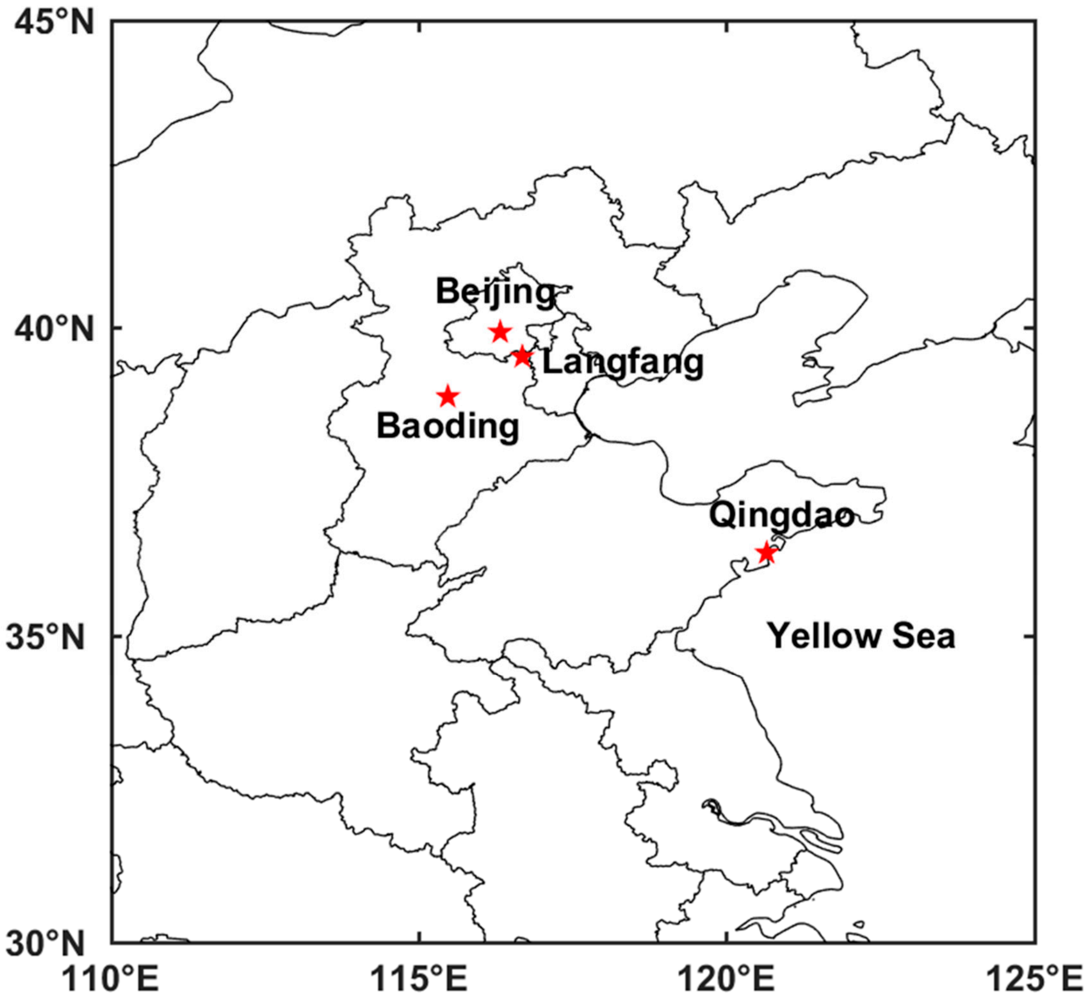

Figure S1. Map of Beijing, Langfang, Baoding, and Qingdao in China.

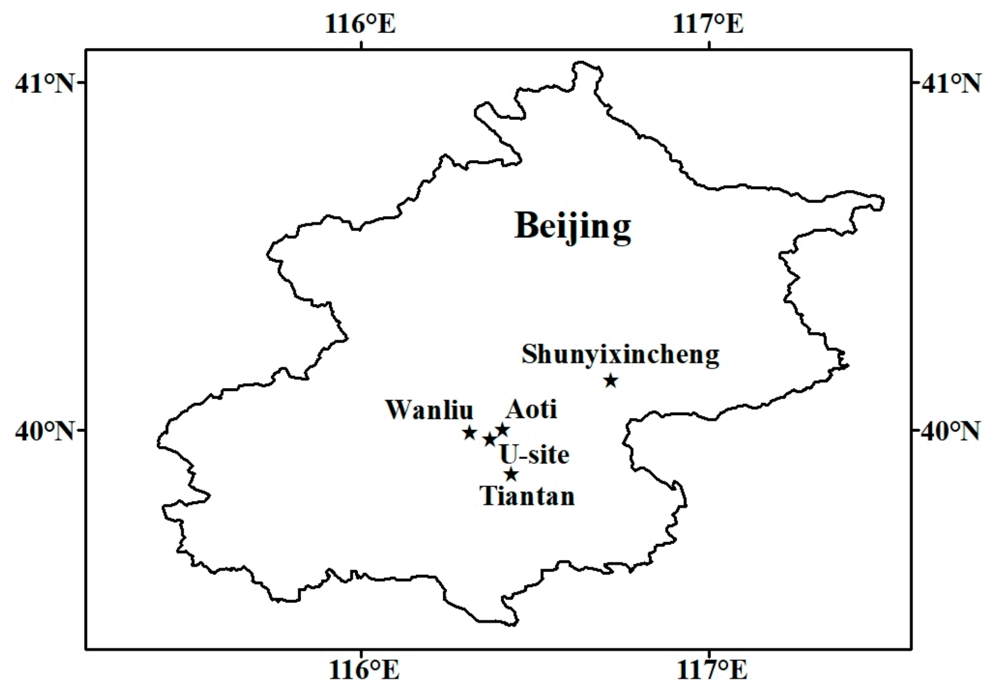

Figure S2. Map of Wanliu, Aoti, Tiantan, Shunyixincheng and U-site in Beijing.

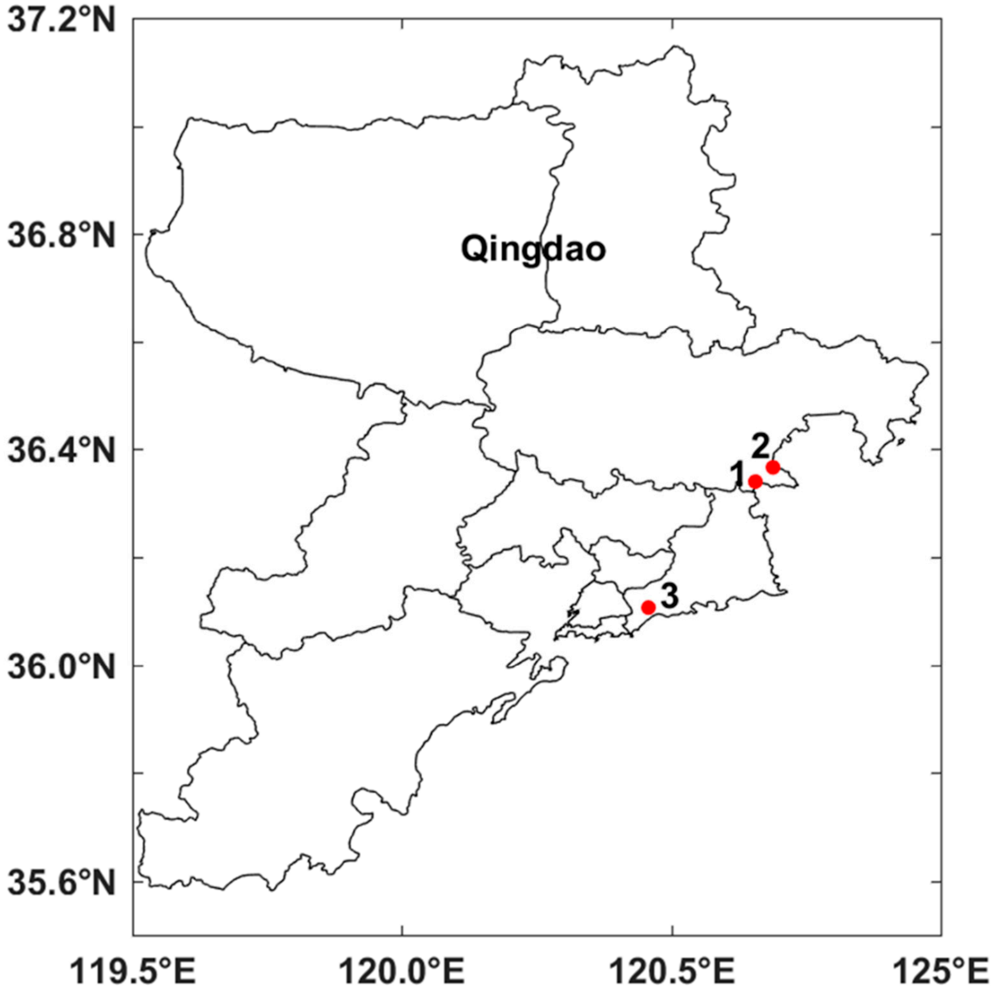

Figure S3. Map of three sampling sites (1), Pilot National Laboratory for Marine Science and Technology (Qingdao) (2), a local air quality monitoring station at Aoshan (3) an air quality monitoring supersite in Qingdao.

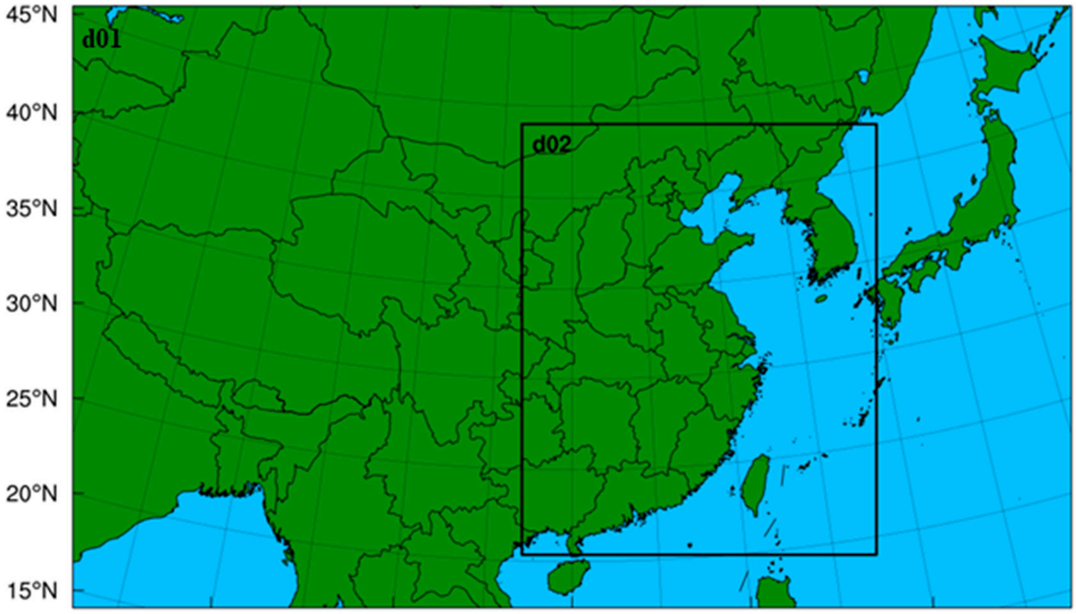

Figure S4. The two domains of meteorological modelling system: Domain 1, a mother domain containing 164 × 97 grid cells at a 36 km spatial resolution for China, and Domain 2, a sub-domain containing 142 × 220 grid cells at a 12 km resolution for eastern China.

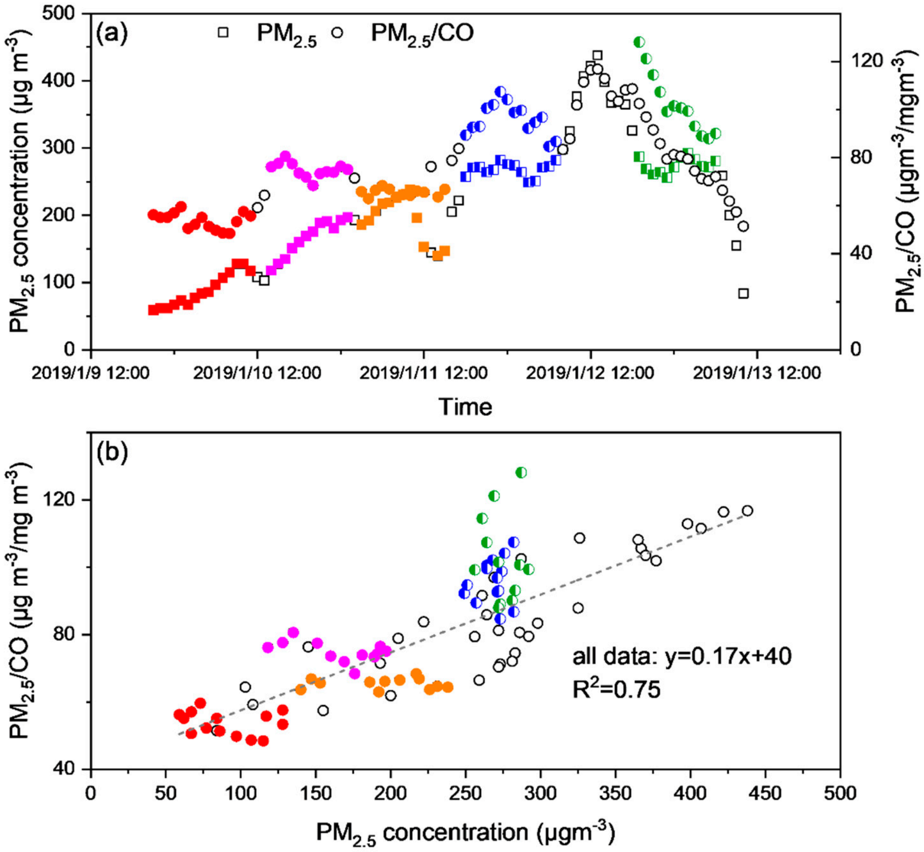

Figure S5. Time series of hourly averages of and the ratios of $PM_{2.5}/CO$ in μg m^{-3}/mg m^{-3} (a) and their correlation (b) on 9–13 January 2019 in Langfang, different color represents specific periods. Red full markers represent data from 21:00 on 9 January to 10:00 on 10 January; pink full markers represent data from 14:00 on 10 January to 01:00 on 11 January; orange full markers represent data from 03:00–12:00 and 14:00–15:00 on 11 January; blue half markers represent data from 18:00 on 11 January to 07:00 on 12 January; green half markers represent data from 19:00 on 12 January to 06:00 on 13 January; empty markers represent the data measured other times.

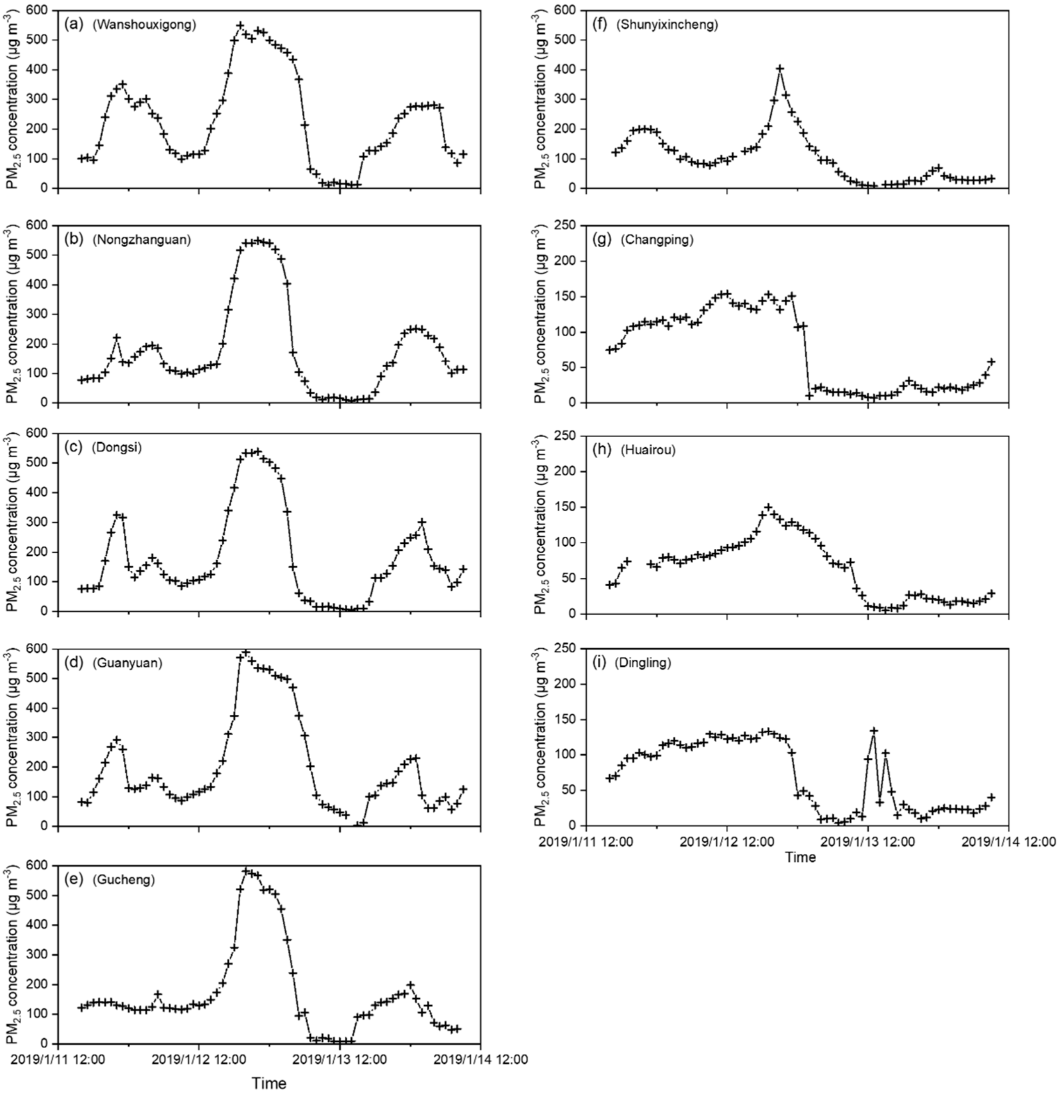

Figure S6. Time series of hourly average mass concentrations of $PM_{2.5}$ measured at nine additional sites in Beijing on 11−14 January 2019.

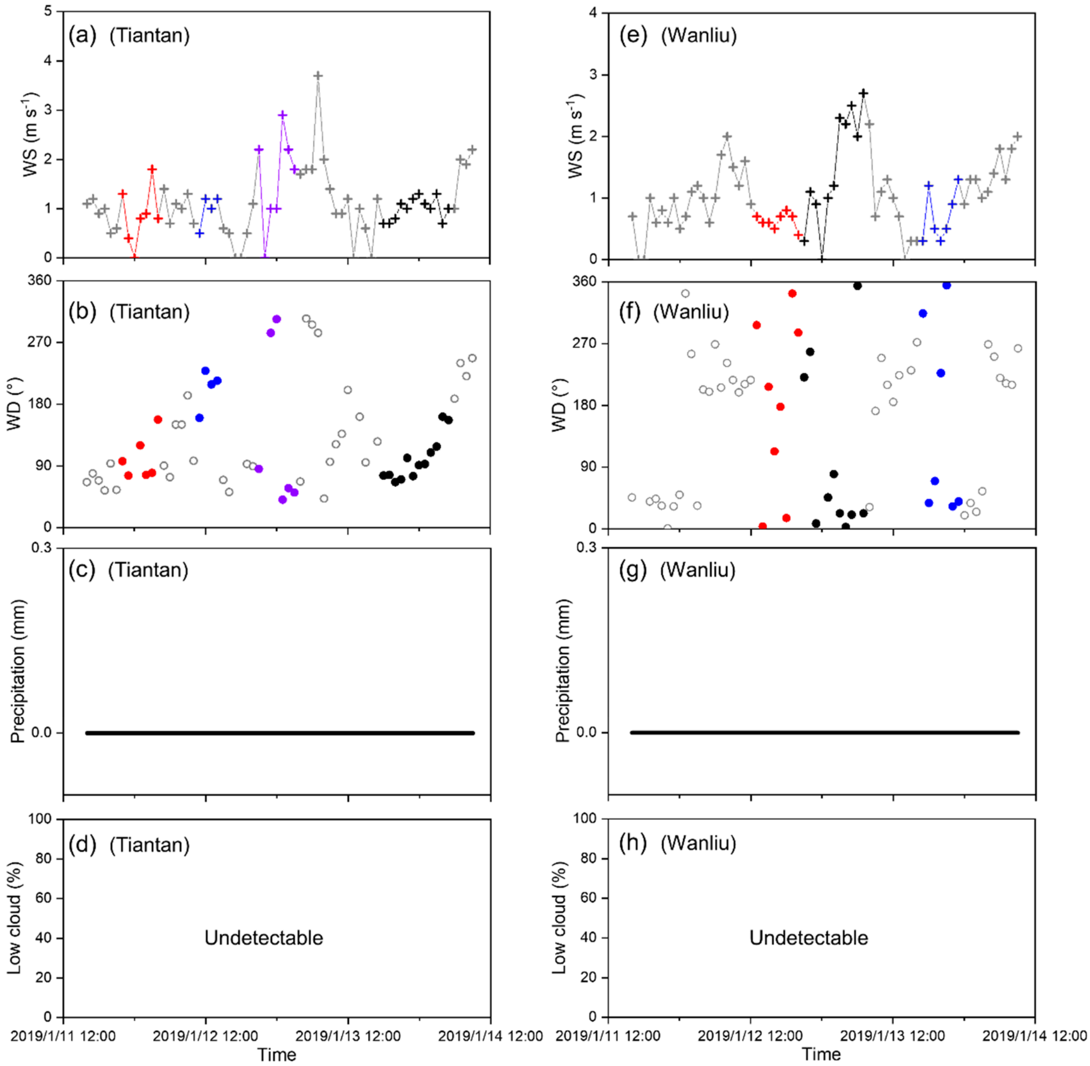

Figure S7. Time series of hourly averages of WS, WD, precipitation, and low cloud percentage at the stations close to Tiantan (a−d) and close to Wanliu (e−f) in Beijing on 11−14 January 2019.

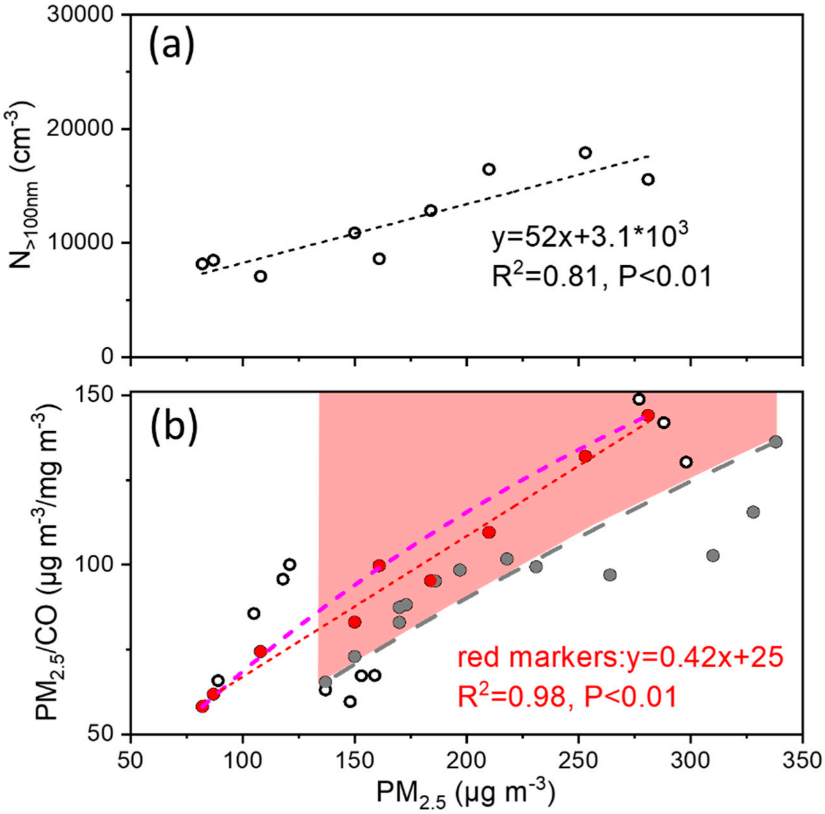

Figure S8. Correlations of $N_{>100}$ and ratios of $PM_{2.5}$/CO in μg m^{-3}/mg m^{-3} with hourly average mass concentrations of $PM_{2.5}$; $N_{>100\ nm}$ (a) and $PM_{2.5}$/CO (b), gray full markers represents data during the decreasing period of $PM_{2.5}$ from 16:00 on 13 January to 04:00 on 14 January; gray dash line represents the theoretical dilution curve using the approach presented in the text, red shallowed area represents the theoretical dilution area in the presence of ambient FMSP; red full markers represent data during the increasing period of $PM_{2.5}$ at 04:00−12:00 on 13 January; pink dash line represents the theoretical mixing curve; empty markers represent the data measured at other times.

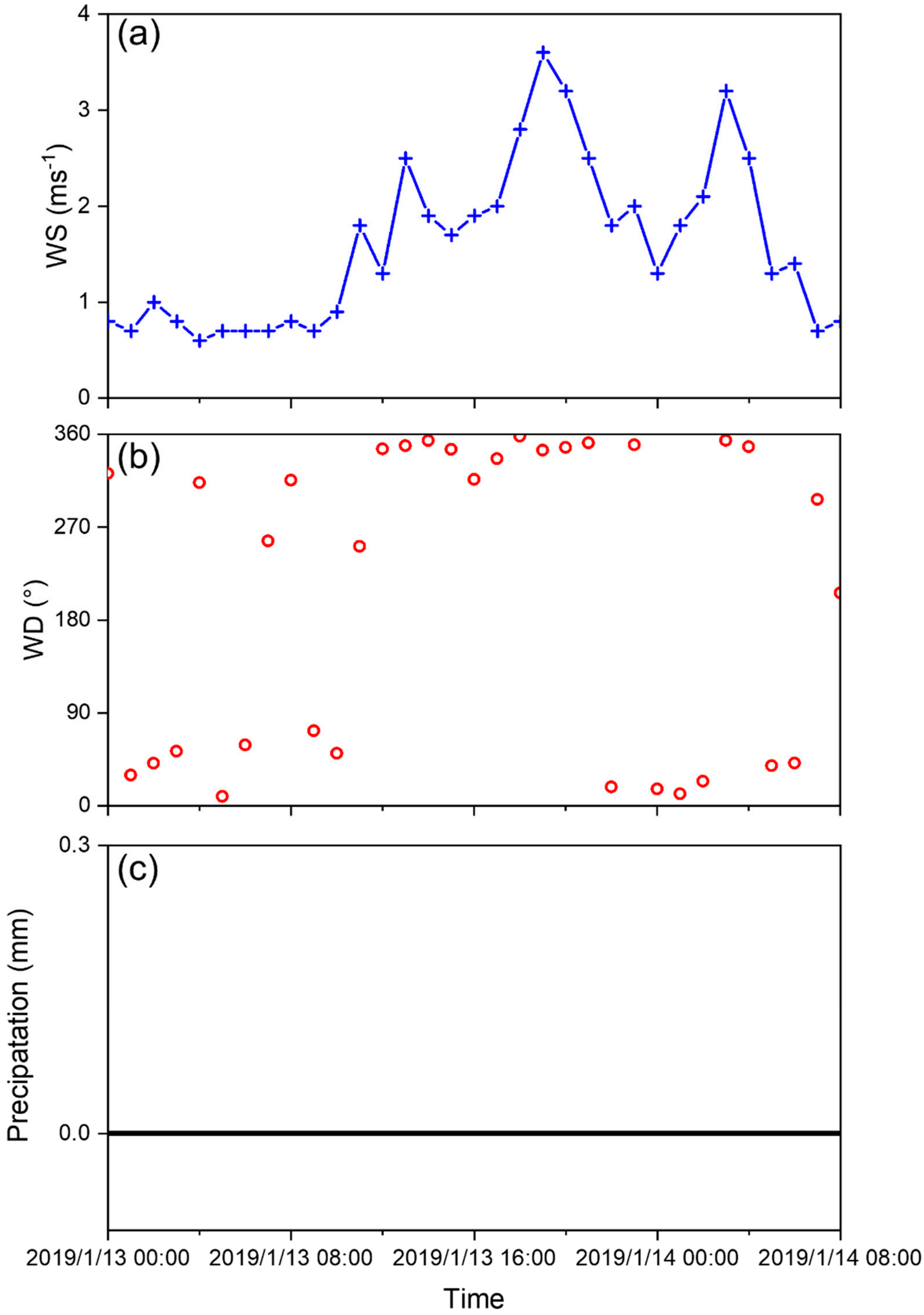

Figure S9. Time series of hourly averages of WS, WD, and precipitation recorded at Aoshan monitoring station in Qingdao.

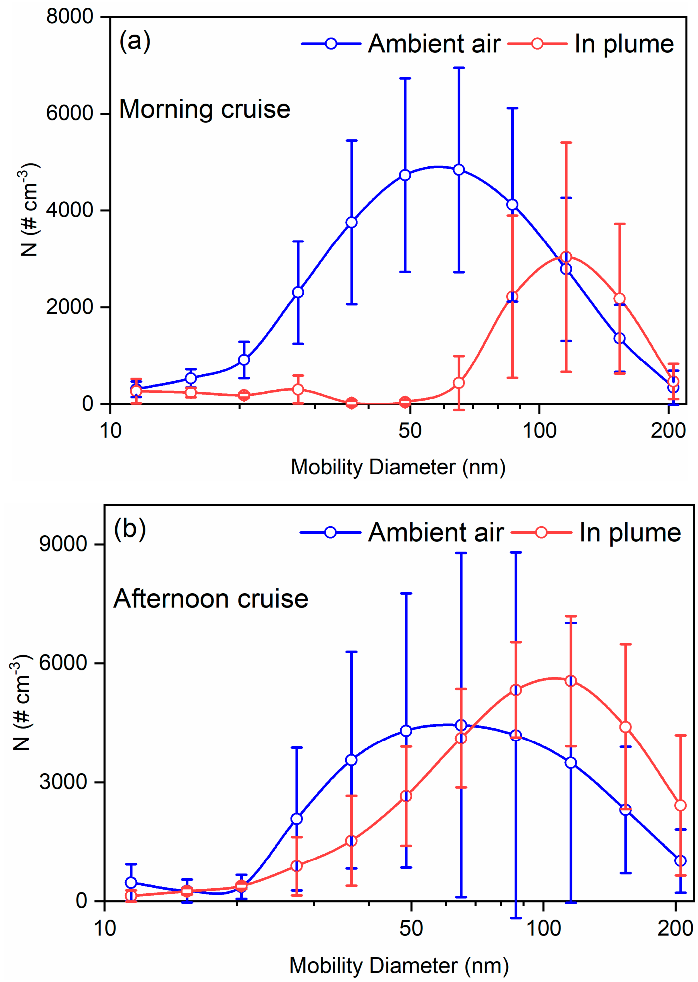

Figure S10. The mean size distributions of particle number concentrations measured by SMPS mounted on UAV in IDSPs and ambient air.

Legends for Videos S1–S6

Video S1. The video was taken on 24 November 2020 in Qingdao, China. The cloud droplets from community house-heating stacks normally survive approximately 20-30 s. The 3 h average RH, wind speed and T were 54 %, 1.7 m/s and 4 ℃, respectively after observing the plume.

Video S2. The video was taken on 2 December 2020 in Qingdao, China. The cloud droplets from community house-heating stacks normally survive approximately 40-50 s. The weather was rainy and the 3 h average RH, wind speed and T were 92 %, 1.7 m/s and 2 ℃, respectively after observing the plume.

Video S3. The video was taken on 27 December 2020 in Qingdao, China. The cloud droplets from community house-heating stacks normally survive approximately 1 min 50 s. The 3 h average RH, wind speed and T were 87 %, 1.0 m/s and 8 ℃, respectively after observing the plume.

Video S4. The video was taken on 28 December 2020 in Qingdao, China. The cloud droplets from community house-heating stacks normally survive approximately 5 min. The 3 h average RH, wind speed and T were 89 %, 1.0 m/s and 7 ℃, respectively after observing the plume.

Video S5. The video was taken on 25 November 2020 in Qingdao, China. The cloud droplets from community house-heating stacks survive approximately 15 s. The 3 h average RH, wind speed and T were 42 %, 1.3 m/s and 8 ℃, respectively after observing the plume.

Video S6. A nano-Scan Particle Sizer on an Unmanned Aerial Vehicle developed in 2017 was used to monitor the particle formation in fresh stack combustion plumes.